RAPID COMMUNICATIONS

PHYSICAL REVIEW FLUIDS **2**, 102602(R) (2017)

Closure theory for the split energy-helicity cascades in homogeneous isotropic homochiral turbulence

Antoine Briard,[1] Luca Biferale,[2] and Thomas Gomez[3,*]

[1]*Sorbonne Universités, UPMC Université Paris 06, UMR 7190, Institut Jean Le Rond d'Alembert, F-75005 Paris, France*

[2]*Department of Physics and INFN, University of Rome "Tor Vergata," Via della Ricerca Scientifica 1, I-00133 Rome, Italy*

[3]*Université Lille Nord de France, F-59000 Lille, France*

(Received 19 July 2017; published 27 October 2017)

We study the energy transfer properties of three-dimensional homogeneous and isotropic turbulence where the nonlinear transfer is altered in a way that helicity is made sign-definite, say, positive. In this framework, known as homochiral turbulence, an adapted eddy-damped quasinormal Markovian closure is derived to analyze the dynamics at very large Reynolds numbers, of order $10^5 \leqslant \mathrm{Re}_\lambda \leqslant 10^6$. In agreement with previous findings, an inverse cascade of energy with a kinetic energy spectrum such as $\propto k^{-5/3}$ is found for scales larger than the forcing one. Conjointly, a forward cascade of helicity towards larger wave numbers is obtained, where the kinetic energy spectrum scales as $\propto k^{-7/3}$. By following the evolution of the closed spectral equations for a very long time and over a huge extension of scales, we found the development of a nonmonotonic shape for the front of the inverse energy flux. The asymptotic temporal scaling laws for the kinetic energy, helicity, and integral scales in both the forced and unforced cases are also determined.

DOI: 10.1103/PhysRevFluids.2.102602

I. INTRODUCTION

Since the discovery that helicity is an inviscid invariant of the three-dimensional (3D) Navier-Stokes equations [1], the possibility of inverse cascades in homogeneous isotropic turbulence (HIT) without mirror symmetry has been greatly investigated: Indeed, two-dimensional turbulence possesses as well two inviscid invariants, kinetic energy and enstrophy, and in this configuration, energy cascades towards large scales [2].

In 3D, the first theoretical considerations date back to the study of Brissaud and co-workers [3], where two different scenarios were proposed: (i) a joint direct cascade of kinetic energy and helicity where $E(k) \sim \epsilon^{2/3}k^{-5/3}$, and $H(k) \sim \epsilon_H\epsilon^{-1/3}k^{-5/3}$, where E and H are the kinetic and helical spectra, and ϵ and ϵ_H the kinetic energy and helicity dissipation rates; and (ii) a split cascade with a direct transfer of helicity combined with an inverse cascade of kinetic energy. In fact, the second scenario was proven to be impossible by Ref. [4] within the eddy-damped quasinormal Markovian (EDQNM) approximation [5–7]. In subsequent papers such as Refs. [8,9] and more recently in Ref. [10], the joint direct cascade of helicity was observed in HIT without mirror symmetry, with strictly zero inverse energy transfer. This stems from the fact that helicity, the scalar product of velocity and vorticity, is not positive-definite, unlike kinetic energy and enstrophy.

Keeping this latter feature in mind, Biferale and co-workers [11,12] performed a "surgery" of the triadic Fourier interactions of turbulence, following the ideas developed by Ref. [13], in order to keep only the ones that maintain sign-definite helicity, yielding to so-called homochiral turbulence. They consequently recovered the second scenario of Ref. [3], namely, an inverse cascade of kinetic energy and a forward cascade of helicity, showing that all three-dimensional turbulent flows indeed possess a subset of Fourier interactions that are potentially able to sustain an inverse energy cascade. Such a

*thomas.gomez@univ-lille1.fr

 ©2017 American Physical Society

"surgery" of the Navier-Stokes equations was thoroughly investigated in multiple subsequent works [14–16] so that the details are not recalled here. The main findings are that by forcing at small scales the decimated Navier-Stokes (dNS) equations where helicity is made sign-definite, say, positive here, kinetic energy is transferred to smaller wave numbers with $E(k) \sim \epsilon^{2/3}k^{-5/3}$. By forcing the dNS equations at large scales, a direct helicity cascade with $E(k) \sim \epsilon_H^{2/3}k^{-7/3}$ was obtained. It was also notably shown that as soon as helicity is not made strictly sign-definite, by adding helical Fourier modes with opposite helicity (negative here), the inverse energy cascade vanishes, and the transition between the upward and forward cascade mechanisms appears to be singular [14,16]. On the other hand, by changing the relative weight of homochiral and heterochiral triads, one is led to a transition from a direct to inverse cascade for a finite value of the control parameter [15], showing that the way Navier-Stokes equations transfer energy across scales might be strongly different by changing the involved degrees of freedom.

Strangely enough, inverse cascades with EDQNM were rarely investigated in the past and mainly for two configurations only: the inverse cascade of kinetic energy in two-dimensional (2D) turbulence [17], and the inverse cascade of magnetic helicity in isotropic magnetohydrodynamics turbulence [18]. Consequently, it appears interesting in terms of modeling to check that a sophisticated model such as EDQNM can handle complex and particular configurations when only specific triadic interactions are kept. In the present Rapid Communication, we aim at further studying these features when helicity is made sign-definite by deriving a different EDQNM model. We show that a split cascade scenario develops and that it can be studied for very large Reynolds numbers and for very long times. In what follows, the adapted EDQNM closure for homochiral turbulence is derived, and then numerical results are presented for cases with and without forcing.

II. EDQNM CLOSURE FOR HOMOCHIRAL TURBULENCE

The spectral counterpart of the Navier-Stokes equation for the fluctuating velocity $\hat{u}_i$ reads in homogeneous isotropic turbulence

$$\left(\frac{\partial}{\partial t} + \nu k^2\right)\hat{u}_j(\boldsymbol{k}) = -i P_{jmn}(\boldsymbol{k}) \int_{\boldsymbol{k}=\boldsymbol{p}+\boldsymbol{q}} u_m(\boldsymbol{p})u_n(\boldsymbol{q})d^3\boldsymbol{p}, \tag{1}$$

where ν is the kinematic viscosity, $i^2 = -1$, the operator $2P_{jmn} = k_m P_{jn} + k_n P_{jm}$, with the projector $P_{jn} = \delta_{jn} - \alpha_j\alpha_n$ and $\alpha_j = k_j/k$, k and $\boldsymbol{k}$ are respectively the wave number and wave vector, and $\hat{(\cdot)}$ denotes the Fourier transform. In isotropic turbulence without reflection symmetry, the spectral second-order velocity-velocity correlation $\hat{R}_{ij}(\boldsymbol{k},t) = \langle \hat{u}_i^*(\boldsymbol{k},t)\hat{u}_j(\boldsymbol{k},t)\rangle$, where $(\cdot)^*$ denotes the complex conjugate and $\langle\cdot\rangle$ an ensemble average, can be decomposed as

$$\hat{R}_{ij}(\boldsymbol{k},t) = \mathcal{E}(\boldsymbol{k},t)P_{ij}(\boldsymbol{k}) + i\epsilon_{ijk}\alpha_k\frac{\mathcal{H}(\boldsymbol{k},t)}{k}, \tag{2}$$

with ϵ_{ijk} the Levi-Civita permutation tensor, and where $\mathcal{E}$ and $\mathcal{H}$ are respectively the kinetic energy and kinetic helicity densities. Such a decomposition involving the kinetic energy density $\mathcal{E}$ and helical density $\mathcal{H}$ was previously used in Refs. [8,9,19]. More recently [10], this decomposition was applied to investigate with EDQNM the large Reynolds numbers dynamics of the kinetic energy and helical spectra defined as

$$E(k,t) = \int_{S_k} \mathcal{E}(\boldsymbol{k},t)d^2\boldsymbol{k}, \quad H(k,t) = \int_{S_k} \mathcal{H}(\boldsymbol{k},t)d^2\boldsymbol{k}, \tag{3}$$

where S_k is a sphere of radius k. The total helicity, which is the scalar product of velocity and vorticity, is then obtained by $\langle \boldsymbol{u}\cdot\boldsymbol{\omega}\rangle/2 = \int_0^\infty H(k,t)dk$. In what follows, we analyze within an adapted EDQNM approximation at large Reynolds numbers, the configuration proposed in Refs. [11,12], namely, the homochiral *decimated Navier-Stokes*.

To select only helical modes of identical sign, the classical Lin equation for $E(k,t)$ [20] and its nonlinear transfer of HIT can no longer be used. One needs another closure, adapted to homochiral turbulence where helicity is made sign-definite. First, the spectral fluctuating velocity is decomposed in positive and negative modes using the helical decomposition [7,13,19] so that

$$\hat{\boldsymbol{u}}(\boldsymbol{k},t) = u_+(\boldsymbol{k},t)\boldsymbol{N}(\boldsymbol{k}) + u_-(\boldsymbol{k},t)\boldsymbol{N}^*(\boldsymbol{k}), \tag{4}$$

where $\boldsymbol{N}$ are the helical modes, which verify $\boldsymbol{N}^*(\boldsymbol{k}) = \boldsymbol{N}(-\boldsymbol{k})$, $\boldsymbol{N}\cdot\boldsymbol{N} = \boldsymbol{0}$, $\boldsymbol{N}\cdot\boldsymbol{N}^* = 2$, and $i\boldsymbol{k}\times\boldsymbol{N} = k\boldsymbol{N}$, so that the spectral fluctuating vorticity reads

$$\hat{\boldsymbol{\omega}}(\boldsymbol{k},t) = k[u_+(\boldsymbol{k},t)\boldsymbol{N}(\boldsymbol{k},t) - u_-(\boldsymbol{k},t)\boldsymbol{N}^*(\boldsymbol{k},t)]. \tag{5}$$

Considering only the positive helical modes, we get for the kinetic energy spectrum

$$E_+(k,t) = \int_{S_k} \mathcal{E}_+(\boldsymbol{k},t)d^2\boldsymbol{k} = \int_{S_k} \langle u_+^*(\boldsymbol{k},t)u_+(\boldsymbol{k},t)\rangle d^2\boldsymbol{k}. \tag{6}$$

Consequently, the helical spectrum is given by $H_+(k,t) = kE_+(k,t)$: This is an exact result, and not a consequence of a maximal helicity condition. The evolution equation of u_+ is obtained by contracting (1) with $N_i^*/2$, which gives

$$\left(\frac{\partial}{\partial t} + \nu k^2\right)u_+(\boldsymbol{k},t) = -\frac{1}{2}i(k_i N_j^*(\boldsymbol{k}) + k_j N_i^*(\boldsymbol{k}))\int_{\boldsymbol{k}=\boldsymbol{p}+\boldsymbol{q}} u_+(\boldsymbol{p})u_+(\boldsymbol{q})N_i(\boldsymbol{p})N_j(\boldsymbol{q})d^3\boldsymbol{p}. \tag{7}$$

The evolution equation of the kinetic energy density $\mathcal{E}_+$ is then

$$\left(\frac{\partial}{\partial t} + 2\nu k^2\right)\mathcal{E}_+(\boldsymbol{k},t) = T_+(\boldsymbol{k},t). \tag{8}$$

It is very important to stress that the nonlinear terms of the Navier-Stokes equations conserve both energy and helicity triad by triad, and therefore the same is true for the dNS. In other words, the nonlinear transfer T_+ is conservative, takes into account triadic interactions of positive helical modes, and reads after some algebra

$$T_+(\boldsymbol{k},t) = \int \mathrm{Re}\big[[k_i N_j^*(\boldsymbol{k}) + k_j N_i^*(\boldsymbol{k})]S_+(\boldsymbol{k},\boldsymbol{p},t)N_i(\boldsymbol{p})N_j(\boldsymbol{q})\big]d^3\boldsymbol{k}, \tag{9}$$

where S_+ is the spectral triple velocity correlation

$$S_+(\boldsymbol{k},\boldsymbol{p},t)\delta(\boldsymbol{k}+\boldsymbol{p}+\boldsymbol{q}) = i\langle u_+(\boldsymbol{k},t)u_+(\boldsymbol{p},t)u_+(\boldsymbol{q},t)\rangle. \tag{10}$$

Then, after some technical manipulations typical of the EDQNM approximation [5,6], one obtains the *decimated Lin equation* of the (positive) kinetic energy spectrum, namely,

$$\left(\frac{\partial}{\partial t} + 2\nu k^2\right)E_+(k,t) = S_+^E(k,t), \tag{11}$$

where the spherically averaged nonlinear transfer is

$$\begin{aligned} S_+^E(k,t) &= \int_{S_k} T_+(\boldsymbol{k},t)d^2\boldsymbol{k} \\ &= 16\pi^2\int_{\Delta_k} k^2pq\theta_{kpq}(1+z)\mathcal{E}_+''\big[p\mathcal{E}_+(y-z)(y+z-2x) \\ &\quad + (1-x-2yz)[k(1+y)\mathcal{E}_+' - p(1+x)\mathcal{E}_+]\big]dpdq, \end{aligned} \tag{12}$$

with Δ_k the domain where k, p, and q are the lengths of the sides of the triangle formed by the triad $\boldsymbol{k}+\boldsymbol{p}+\boldsymbol{q} = \boldsymbol{0}$, and where x, y, and z are the cosines of the angles formed by $\boldsymbol{p}$ and $\boldsymbol{q}$, $\boldsymbol{q}$ and $\boldsymbol{k}$, and $\boldsymbol{k}$ and $\boldsymbol{p}$, respectively. For the sake of clarity, $\mathcal{E}_+ = E_+(k,t)/4\pi k^2$, $\mathcal{E}_+' = E_+(p,t)/4\pi p^2$, and $\mathcal{E}_+'' = E_+(q,t)/4\pi q^2$. The characteristic time θ_{kpq} of the triple correlations contains the eddy-damping term given by $A_1\sqrt{\int_0^k x^2E_+(x,t)dx}$, and similarly for wave numbers p and q. In fully isotropic turbulence, to get a Kolmogorov constant $C_K \simeq 1.4$, one usually chooses $A_1 = 0.355$ [10,18,21,22]. In order not to arbitrarily modify A_1, we keep this value for the present work: The impact of changing A_1 is discussed later on. Note that since in homochiral turbulence one has $H_+ = kE_+$, the eddy-damping term can be written directly as a function of the helical spectrum, $A_1\sqrt{\int_0^k xH_+(x,t)dx}$. The previous equations of the EDQNM closure for the sign-definite helicity originating from the decimated Navier-Stokes equation are the main theoretical contributions of this work.

It is worth mentioning that S_+^E can be obtained in a different way: Starting from the full helical system within the EDQNM framework [4,10], one can replace the kinetic and helical spectra E and H by respectively $(E_+ + E_-)$ and $k(E_+ - E_-)$; this would then yield (12) by setting $E_- = 0$. Proceeding in this way is much more complex than the direct approach proposed here. The influence of negative modes is discussed in the Conclusion.

In what follows, we wish to recover two features of homochiral turbulence: (i) the direct helicity cascade of Ref. [12] where the kinetic energy spectrum scales as $E_+(k) \sim {\epsilon_H}^{2/3}k^{-7/3}$, and (ii) the inverse cascade of energy in $E_+(k) \sim \epsilon^{2/3}k^{-5/3}$. For the EDQNM simulations, the wave-number space is discretized using a logarithmic mesh $k_{i+1} = rk_i$ for $i = 1,\dots,n$, where n is the total number of modes and $r = 10^{1/f}$, $f = 15$ being the number of points per decade. It has been checked that increasing f, for instance, up to $f = 20$, does not modify the slopes of the spectra, nor the asymptotic values of the integrated quantities (as kinetic energy) more than 1%. This mesh spans from $k_{\min} = 10^{-6}k_L$ to $k_{\max} = 10k_\eta$, where k_L is the integral wave number and $k_\eta = (\epsilon/\nu^3)^{1/4}$ the Kolmogorov wave number. The initial kinetic energy spectrum is given by $E_+(k) \sim k^\sigma \exp(-\sigma k^2/2)$, where the infrared slope is $\sigma = 2$, corresponding to Saffman turbulence. Simulations not presented here revealed that the results of this work are independent of the infrared slope, in particular, the findings are the same for Batchelor turbulence ($\sigma = 4$). The initial E_+ is normalized so that $\langle u_+^2\rangle = \int_0^\infty E_+(k)dk$ is unit at $t = 0$.

III. RESULTS AT LARGE REYNOLDS NUMBERS

First, homogeneous homochiral turbulence without any forcing is considered. The $k^{-7/3}$ scaling is recovered in Fig. 1(a) at large Reynolds numbers, which corresponds to the forward helicity cascade [3]: This inertial $k^{-7/3}$ range grows with time and spans more than four decades at the largest Reynolds number. The noteworthy feature is that even without forcing, if large Reynolds numbers are reached, strong inverse transfer mechanisms occur since the peak of E_+ increases with time, unlike in fully isotropic decaying turbulence. Further evidence for intense inverse nonlocal transfers is that, even though the infrared scaling of the kinetic energy spectrum is initially $E_+(k < k_L) \sim k^2$, it rapidly becomes $E_+(k_L/10 < k < k_L) \sim k^4$, close to the integral wave number, which is a signature of strong back transfers [21–24]. It follows from $E_+(k) \sim k^{-7/3}$ that the helical spectrum scales in $H_+(k) = kE_+(k) \sim {\epsilon_H}^{-2/3}k^{-4/3}$.

In addition, one can remark from Fig. 1(a) that the peak of the kinetic energy spectrum E_+^{peak} evolves as k^{-1} with time. This has nothing to do with inertial range scaling considerations, since the $k^{-7/3}$ inertial scaling of the direct helicity cascade can be observed for any given time. The time evolution scaling of E_+^{peak} can be justified as follows: Since we mainly have a direct helicity cascade, one can roughly assume that $\epsilon \simeq 0$, consistently with arguments given in Ref. [3]. Thus, it follows that the kinetic energy $\langle u_+^2\rangle$, whose evolution is given by $\partial_t\langle u_+^2\rangle = -\epsilon \simeq 0$, remains constant, which is well verified numerically [see later in Fig. 3(b)]. Hence, using the definition of the kinetic energy, one can assume that it is mainly given by the integral scale,

$$\langle u_+^2\rangle = \int_0^\infty E_+(k,t)dk \simeq \int_0^{k_L} E_+^{\text{peak}}(t)dk = k_L E_+^{\text{peak}}(t). \tag{13}$$

The kinetic energy being constant, one obtains that the time evolution of the kinetic energy spectrum peak is given by $E_+^{\text{peak}}(t) \sim {k_L}^{-1}(t)$. We make no claim that in the unforced case there is an inverse

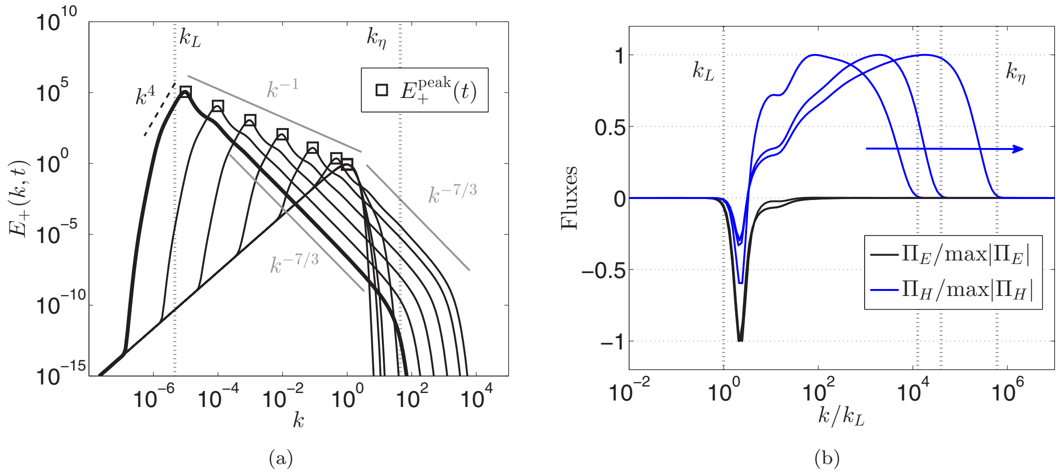

FIG. 1. Time evolution of spectra and fluxes for Saffman turbulence ($\sigma = 2$): The integral and Kolmogorov wave numbers k_L and k_η are displayed as vertical dashed lines. (a) $E_+(k,t)$ for various times $t = 0$, $t = 0.1\tau_0$, $t = 0.5\tau_0$, and $t = 10^n\tau_0$ for $n \in [1;6]$, where τ_0 is the eddy turnover time: k_L and k_η correspond to the last time (thick spectrum) where $\mathrm{Re}_\lambda(t = 10^6\tau_0) = 10^6$. The position of the peak of energy $E_+^{\rm peak}$ is indicated by $\square$ to visualize its time evolution. (b) Kinetic (black) and helical (blue) fluxes Π_E and Π_H for various times $t/\tau_0 = [10; 10^2; 10^4]$. For better readability, fluxes are normalized by their maximum value and presented as functions of k/k_L.

cascade with a k^{-1} scaling, we simply derived a scaling law for the time evolution of $E_+^{\rm peak}(t)$. The time evolution of $\langle u_+^2\rangle$ in the forced case, quite different from the unforced situation, is analyzed later on, along with the integral scales.

In Fig. 1(b) we show the evolution of the two fluxes, Π_E and Π_H, where $\Pi_E(k) = -\int_0^k S_+^E(x)dx$ and $\Pi_H(k) = -\int_0^k x S_+^E(x)dx$. As stated earlier, both energy and helical transfers with homochiral triadic interactions are conservative: Indeed, one has $\Pi_E(k \to \infty) = \Pi_H(k \to \infty) = 0$. Furthermore, there is a direct cascade of helicity since Π_H is mostly positive in the inertial range and spans more and more decades with time, which is consistent with the $k^{-7/3}$ scaling of E_+ of Fig. 1(a). In addition, Fig. 1(b) illustrates that there is an inverse transfer occurring on a small range around k_L for E_+.

So far, it has been shown that without any forcing, there is a direct cascade of helicity as $E_+(k) \sim k^{-7/3}$, that the kinetic energy remains constant, and as a consequence the peak of energy increases with time as $E_+^{\rm peak}(t) \sim k^{-1}$.

To increase the scaling region of the inverse cascade, we add to the decimated Lin equation (11) a forcing term $F(k)$, to have the possibility to study the split cascade scenario with a well developed inverse energy transfer for asymptotically long times. The forcing term is given by

$$F(k) = C_1 \exp\left(-\frac{1}{(C_2)^2}\left[\ln\left(\frac{k}{k_f}\right)\right]^2\right), \tag{14}$$

with C_1, so that one has $\int_0^\infty F(k)dk = 1$, $C_2 = 0.1$, and $k_f = 1$, as proposed in Ref. [10]. We double checked that the following numerical results are independent of the forcing term by studying also the case with $F(k) \sim k^4 \exp(-2k^2)$ (not shown). The time evolution of the kinetic energy spectrum is shown in Fig. 2(a), where the forcing term F is in gray. It is clear that the system develops a split cascade on both sides of the forcing term. Indeed, as time increases, a $k^{-5/3}$ range grows at large scales, similar to the one obtained in Ref. [11], which is strong evidence for the inverse cascade of kinetic energy. However, for wave numbers larger than k_f, the $k^{-7/3}$ range is preserved, as in Fig. 1(a) without forcing. It is important to stress that this is where the split energy-helicity

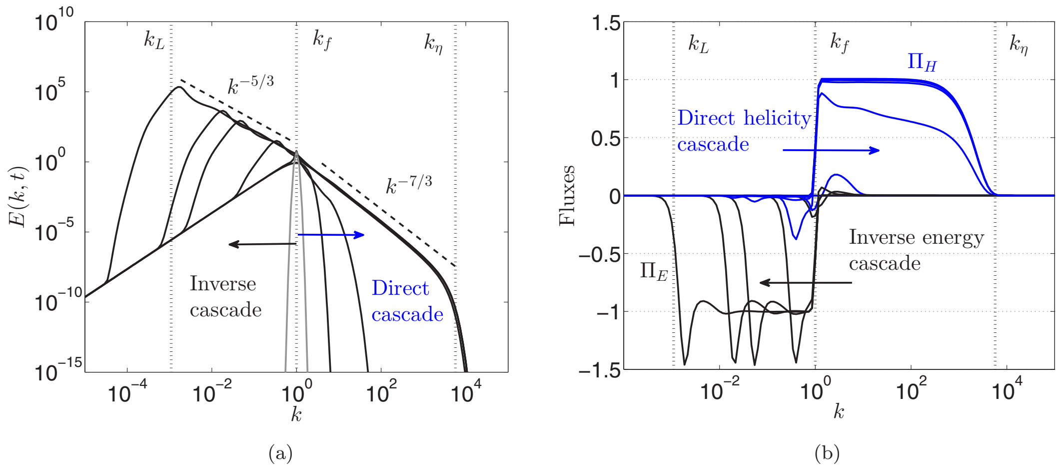

FIG. 2. Time evolution of the kinetic energy spectrum, and kinetic and helical fluxes for Saffman turbulence ($\sigma = 2$), from $t = 0$ to $t = 500\tau_0$, where the curves are sampled at $t/\tau_0 = 0; 1; 10; 50; 100; 500$. The integral, forcing, and Kolmogorov wave numbers k_L, k_f, and k_η are displayed as vertical dashed lines at $\mathrm{Re}_\lambda(t = 500\tau_0) = 3 \times 10^5$. (a) $E_+(k,t)$ with the forcing term $F(k)$ (gray) defined in (14). (b) Kinetic (black) and helical (blue) fluxes Π_E and Π_H.

simultaneous cascade is observed: This is notably due to the fact that by using EDQNM we can push the resolution on both sides to very large values.

The kinetic and helical fluxes Π_E and Π_H are presented in Fig. 2(b). For $k > k_f$, at scales smaller than the forcing one, the helical flux is positive, indicating a direct cascade of helicity. For $k < k_f$, the helical flux is zero and the kinetic one Π_E is negative, showing a stable inverse cascade of energy for scales larger than the forcing one. Note that the shape of Π_E is qualitatively in agreement with the one of Ref. [15] (Fig. 3 therein, curve marked with squares). Here, we show in a clean way that the inverse transfer has a nontrivial wavy shape around the front: This is very likely because of the strong variations of E_+ around k_L. The wavy shape is not a consequence of a too low resolution: Indeed, from 10 to 20 points per decade, the shape persists, with only slight variations in intensity. The numerical evidence for the split energy cascade in Fig. 2(b) further justifies that for $k < k_f$ the kinetic energy depends only on ϵ (since Π_H is almost zero), and that E_+ and H_+ only depend on ϵ_H for $k > k_f$ (since Π_E is almost zero). Compensated kinetic energy spectra are presented in Fig. 3(a) in the direct and inverse cascades. A reasonable plateau is obtained in both cases spanning two decades. In the inverse cascade, $E_+(k)k^{5/3}\epsilon^{-2/3}$ settles around 3.35, and $E_+(k)k^{7/3}{\epsilon_H}^{-2/3}$ around 2.7 in the direct cascade. Both constants are larger than the Kolmogorov one in HIT. For the constant of the inverse cascade, this is somehow consistent with constants of inverse energy cascades found in two-dimensional turbulence which are roughly between 6 and 10 [25,26].

Note that the values of the constants could be modified by changing the eddy-damping parameter A_1. So far, we chose $A_1 = 0.355$ because this is the value commonly used in EDQNM for isotropic turbulence with and without helicity, which is relevant also for 2D turbulence [17]. Here, more specifically, the plateau $E_+(k)k^{5/3}\epsilon^{-2/3}$ in the inverse cascade increases with larger eddy-damping constants, from 2.3 ($A_1 = 0.2$) to 4.2 ($A_1 = 0.49$, value used in Ref. [27]). The value 4.2 for the plateau of the inverse cascade is very close to what is obtained in Ref. [11]. To obtain for $E_+(k)k^{5/3}\epsilon^{-2/3}$ a constant around 6 as in 2D turbulence, one would need to go up to $A_1 = 0.8$.

About one-point statistics. Finally, we investigate the time evolution of some one-point statistics for both the forced and unforced cases, in order to show that the dynamics is very different. We focus on the kinetic energy $K = \langle u_+^2 \rangle$, the kinetic integral scale $L = 1/k_L = 3\pi/(4K)\int_0^\infty (E_+(k)/k)dk$, helicity $K_H = \langle u_+ \omega_+ \rangle$, and the helical integral scale L_H, defined analogously to L.

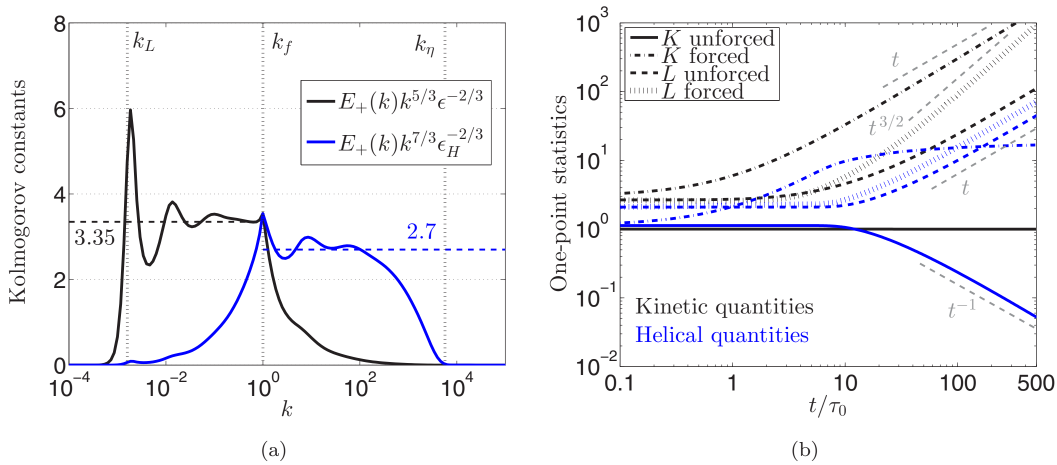

FIG. 3. (a) Compensated kinetic energy spectra in the inverse (black) and direct (blue) cascades. The integral, forcing, and Kolmogorov wave numbers k_L, k_f, and k_η are displayed as vertical dashed lines at $\mathrm{Re}_\lambda(t = 500\tau_0) = 3 \times 10^5$. (b) Time evolution of kinetic energy K and integral scale L (black), and helicity K_H and helical integral scale L_H (blue) for the forced and unforced cases. The gray dashed curves indicate the power laws t, t^{-1}, and $t^{3/2}$; K for the forced case has been increased by a factor 3 for readability reasons.

For the unforced case, the constancy of the kinetic energy K arises from $\epsilon \simeq 0$ in the direct helicity cascade. Then, from a dimensional analysis $L \sim K^{3/2}/\epsilon$, with $\epsilon = -\partial_t K$, it follows that $L \sim t$. Moreover, it is obtained numerically that the temporal evolution of the two integral scales is similar, $L \sim L_H$, as in the fully nonlinear helical configuration [10]. But for unforced homochiral turbulence, one has $L \sim t$ instead of the classical law $\sim t^{2/(\sigma+3)}$. One can then deduce, again from a dimensional analysis, that $K_H \sim K/L_H \sim t^{-1}$.

For the forced configuration, the dynamics is driven by the inverse energy cascade: ϵ is constant and therefore the kinetic energy grows linearly with time as $K \sim \epsilon t$, as in 2D [17]. From a dimensional analysis, it follows that $L \sim K^{3/2}/\epsilon \sim t^{3/2}$. Now, at difference with the unforced case and the full nonlinear helical problem, L and L_H evolve differently: L_H belongs to the inverse energy cascade range where $\epsilon_H \simeq 0$. This is the opposite of the previous configuration where L was falling into the range where $\epsilon \simeq 0$. Consequently, the helical integral scale should evolve as $L_H \sim t$. Finally, helicity is still given by K/L_H so that K_H should be constant. One could conclude that in the forced case, helicity behaves as kinetic energy in the unforced case.

All these temporal scaling laws for both the unforced and forced cases are well assessed in Fig. 3(b), after a transient regime of about 20 turnover times.

IV. CONCLUSIONS

In conclusion, we addressed a particular kind of helical turbulence, where only specific triadic interactions are kept, so that the helicity is made sign-definite. In this particular homochiral framework, the 3D turbulence possesses two sign-definite inviscid invariants, namely, kinetic energy and helicity, similarly to 2D turbulence with kinetic energy and enstrophy. The main objective of this study was to show that a spectral closure method, such as EDQNM, could recover the main findings of Refs. [11,12]. To do so, an adapted EDQNM approximation was derived, taking into account only the particular interactions that make helicity sign-definite (positive here). The direct helicity cascade, where $E_+(k) \sim {\epsilon_H}^{2/3} k^{-7/3}$, is first obtained in unforced homochiral turbulence, where the kinetic energy flux $\epsilon \simeq 0$. In such a configuration, the kinetic energy K remains constant, helicity decays as $K_H \sim t^{-1}$, and the kinetic and helical integral scales grow linearly as $L \sim L_H \sim t$. With a forcing term, in addition to the helicity forward cascade, an inverse energy cascade develops toward smaller wave numbers, where the helicity flux $\epsilon_H \simeq 0$. In this regime of forced homochiral turbulence, dynamically driven by the inverse cascade, the kinetic energy evolves linearly with time as $K \sim \epsilon t$, and the integral scale as $L \sim t^{3/2}$; but now, since $\epsilon_H \simeq 0$ in the inverse cascade of energy, one has $L_H \sim t$ and a constant helicity using $K_H \sim K/L_H$.

Our work shows the possibility to have a stable split cascade in three-dimensional turbulence under a strong restriction of the helical interactions within the EDQNM framework. It remains to be understood how much this phenomenology might be indeed observed in more realistic flow configurations, as in the presence of strong rotation or confinement, where a transition from direct to inverse energy cascade is also observed [28–32].

It will be also crucial to further test the robustness of the phenomenon in the presence of helical modes of the other sign. Direct numerical simulations have shown that switching on heterochiral triads might play a singular role for the direction of the energy cascade [14,15,33]. It remains to be tested if this is also verified within the EDQNM approximation. It might be interesting as well to study the inverse cascade regime in the presence of a large scale drag, in order to allow for the formation of a large scale stationary condensate [34]. At difference from the two-dimensional case, the condensate will necessarily have strong helical properties and be close to an ABC quasistationary solution of the three-dimensional Navier-Stokes equations [35–37]. Works in this direction will be reported elsewhere. Finally, it is important to stress that similar EDQNM studies can be extended to helical magnetohydrodynamics (MHD) [38,39].

ACKNOWLEDGMENT

The research leading to these results has received funding from the European Union's Seventh Framework Programme (FP7/2007-2013) under Grant Agreement No. 339032.

[1] H. K. Moffatt, The degree of knottedness of tangled vortex lines, J. Fluid Mech. **35**, 117 (1969).
[2] G. Boffetta and R. E. Ecke, Two-dimensional turbulence, Annu. Rev. Fluid Mech. **44**, 427 (2012).
[3] A. Brissaud, U. Frisch, J. Leorat, M. Lesieur, and A. Mazure, Helicity cascades in fully developed isotropic turbulence, Phys. Fluids **16**, 1366 (1973).
[4] J. C. André and M. Lesieur, Influence of helicity on the evolution of isotropic turbulence at high reynolds number, J. Fluid Mech. **81**, 187 (1977).
[5] S. A. Orszag, Analytical theories of turbulence, J. Fluid Mech. **41**, 363 (1970).
[6] M. Lesieur, *Turbulence in Fluids*, 4th ed. (Springer, Dordrecht, 2008).
[7] P. Sagaut and C. Cambon, *Homogeneous Turbulence Dynamics* (Cambridge University Press, Cambridge, U.K., 2008).
[8] V. Borue and S. A. Orszag, Spectra in helical three-dimensional homogeneous isotropic turbulence, Phys. Rev. E **55**, 7005 (1997).
[9] Q. Chen, S. Chen, and G. L. Eyink, The joint cascade of energy and helicity in three-dimensional turbulence, Phys. Fluids **15**, 361 (2003).
[10] A. Briard and T. Gomez, Dynamics of helicity in homogeneous skew-isotropic turbulence, J. Fluid Mech. **821**, 539 (2017).
[11] L. Biferale, S. Musacchio, and F. Toschi, Inverse Energy Cascade in Three-Dimensional Isotropic Turbulence, Phys. Rev. Lett. **108**, 164501 (2012).
[12] L. Biferale, S. Musacchio, and F. Toschi, Split energy–helicity cascades in three-dimensional homogeneous and isotropic turbulence, J. Fluid Mech. **730**, 309 (2013).
[13] F. Waleffe, The nature of triad interactions in homogeneous turbulence, Phys. Fluids **4**, 350 (1992).
[14] G. Sahoo, F. Bonaccorso, and L. Biferale, Role of helicity for large- and small-scale turbulent fluctuations, Phys. Rev. E **92**, 051002(R) (2015).

[15] G. Sahoo, A. Alexakis, and L. Biferale, Discontinuous Transition from Direct to Inverse Cascade in Three-Dimensional Turbulence, Phys. Rev. Lett. **118**, 164501 (2017).

[16] G. Sahoo, M. De Pietro, and L. Biferale, Helicity statistics in homogeneous and isotropic turbulence and turbulence models, Phys. Rev. Fluids **2**, 024601 (2017).

[17] A. Pouquet, M. Lesieur, J. C. André, and C. Basdevant, Evolution of high Reynolds number two-dimensional turbulence, J. Fluid Mech. **72**, 305 (1975).

[18] A. Pouquet, U. Frisch, and J.-L. Léorat, Strong MHD helical turbulence and the nonlinear dynamo effect, J. Fluid Mech. **77**, 321 (1976).

[19] C. Cambon and L. Jacquin, Spectral approach to non-isotropic turbulence subjected to rotation, J. Fluid Mech. **202**, 295 (1989).

[20] T. von Kármán and C. C. Lin, On the concept of similarity in the theory of isotropic turbulence, Rev. Mod. Phys. **21**, 516 (1949).

[21] M. Lesieur and S. Ossia, 3D isotropic turbulence at very high Reynolds numbers: EDQNM study, J. Turbulence **1**, N7 (2000).

[22] A. Briard, T. Gomez, P. Sagaut, and S. Memari, Passive scalar decay laws in isotropic turbulence: Prandtl number effects, J. Fluid Mech. **784**, 274 (2015).

[23] G. L. Eyink and D. J. Thomson, Free decay of turbulence and breakdown of self-similarity, Phys. Fluids **12**, 477 (2000).

[24] M. Meldi and P. Sagaut, On non-self-similar regimes in homogeneous isotropic turbulence decay, J. Fluid Mech. **711**, 364 (2012).

[25] R. H. Kraichnan, Inertial-range transfer in two- and three-dimensional turbulence, J. Fluid Mech. **47**, 525 (1971).

[26] U. Frisch and P. L. Sulem, Numerical simulation of the inverse cascade in two-dimensional turbulence, Phys. Fluids **27**, 1921 (1984).

[27] W. J. T. Bos, L. Chevillard, J. F. Scott, and R. Rubinstein, Reynolds number effect on the velocity increment skewness in isotropic turbulence, Phys. Fluids **24**, 015108 (2012).

[28] P. D. Mininni and A. Pouquet, Helicity cascades in rotating turbulence, Phys. Rev. E **79**, 026304 (2009).

[29] A. Celani, S. Musacchio, and D. Vincenzi, Turbulence in More than Two and Less than Three Dimensions, Phys. Rev. Lett. **104**, 184506 (2010).

[30] H. Xia, D. Byrne, G. Falkovich, and M. Shats, Upscale energy transfer in thick turbulent fluid layers, Nat. Phys. **7**, 321 (2011).

[31] F. S. Godeferd and F. Moisy, Structure and dynamics of rotating turbulence: A review of recent experimental and numerical results, Appl. Mech. Rev. **67**, 030802 (2015).

[32] L. Biferale, F. Bonaccorso, I. M. Mazzitelli, M. A. T. van Hinsberg, A. S. Lanotte, S. Musacchio, P. Perlekar, and F. Toschi, Coherent Structures and Extreme Events in Rotating Multiphase Turbulent Flows, Phys. Rev. X **6**, 041036 (2016).

[33] A. Alexakis, Helically decomposed turbulence, J. Fluid Mech. **812**, 752 (2017).

[34] M. Chertkov, C. Connaughton, I. Kolokolov, and V. Lebedev, Dynamics of Energy Condensation in Two-Dimensional Turbulence, Phys. Rev. Lett. **99**, 084501 (2007).

[35] T. Dombre, U. Frisch, J. M. Greene, M. Hénon, A. Mehr, and A. M. Soward, Chaotic streamlines in the ABC flows, J. Fluid Mech. **167**, 353 (1986).

[36] H. K. Moffatt, Helicity and singular structures in fluid dynamics, Proc. Natl. Acad. Sci. U.S.A. **111**, 3663 (2014).

[37] G. Sahoo and L. Biferale, Disentangling the triadic interactions in Navier-Stokes equations, Eur. Phys. J. E **38**, 114 (2015).

[38] A. Alexakis, Two-dimensional behavior of three-dimensional magnetohydrodynamic flow with a strong guiding field, Phys. Rev. E **84**, 056330 (2011).

[39] M. Linkmann, G. Sahoo, M. McKay, A. Berera, and L. Biferale, Effects of magnetic and kinetic helicities on the growth of magnetic fields in laminar and turbulent flows by helical Fourier decomposition, Astrophys. J. **836**, 26 (2017).